TELKOMNIKA Telecommunication, Computing, Electronics and Control
Vol. 18, No. 6, December 2020, pp. 3116~3122
ISSN: 1693-6930, accredited First Grade by Kemenristekdikti, Decree No: 21/E/KPT/2018
DOI: 10.12928/TELKOMNIKA.v18i6.16426

Low cost, high performance fuel cell energy conditioning system controlled by neural network

Fredy H. Martínez S., Fernando Martínez S., Holman Montiel Ariza
Facultad Tecnológica, Universidad Distrital Francisco José de Caldas, Colombia

Article Info

Article history:

Received Apr 18, 2020
Revised Jun 17, 2020
Accepted Jul 9, 2020

Keywords:

Boost converter
Continuous conduction mode
Energy conditioning system
Fuel cell
Neural network

ABSTRACT

Fuel cells are an important option for the generation of renewable, efficient and environmentally friendly electricity. Although there are commercial applications in the industrial, residential and automotive sectors, it is not yet a mature technology and requires much research, particularly to reduce its costs to a level competitive with other technologies. This research is currently focused not only on the structure of the cell but also on the additional elements and subsystems required for its implementation as an energy solution. In this article, we propose an electrical energy conditioning scheme for the Formic acid fuel cell (direct formic acid fuel cell or DFAFC). This fuel cell was selected for its high performance, and low cost in low and medium power applications. The proposed system consists of a direct current-direct current (DC-DC) regulator supported by a power converter controlled by a Cortex-M3 ARM processor. This CPU is used to propagate a static neural network trained with the non-linear dynamics of the power converter. The power circuit is modeled and simulated to produce the training parameters. The neural network is trained externally and runs off-line on the processor. The results show not only the regulation capacity of the control scheme but also its response speed to sudden changes in the load.

Corresponding Author:

Fredy H. Martínez S.,
Facultad Tecnológica,
Universidad Distrital Francisco José de Caldas,
Cll 68 D Bis A Sur no. 49F – 70, Bogotá D.C, Colombia.
Email: fhmartinezs@udistrital.edu.co

1. INTRODUCTION

The current demand for fuel cells, as well as other sustainable sources of energy, is growing, which drives its research and development [1-3]. But in particular, fuel cells are very interesting given their capacity for continuous and reliable supply, and their low emission of pollutants into the environment. A fuel cell is an electrochemical device capable of continuously producing electrical current. The fuel cell is fed with a continuous flow of fuel and oxidant which, thanks to a controlled chemical reaction, generates electrical energy [4]. Due to its principle of operation, the fuel cell produces electrical energy in a similar way to a battery. However, unlike it, the fuel cell has a continuous supply of chemical reagents, so it does not wear out (nor do its catalytic electrodes) and must not be replaced every time its chemical reaction is exhausted (this simply does not happen). Fuel cells can process different types of reducers and oxidants [5, 6]. A reducer is a substance that can be oxidized (hence the need for the oxidant) during a controlled chemical reaction, and thus continuously produce the anode required by the cell. In line with the reductant, the oxidant is selected in a suitable way for the chemical reaction. The continuous supply of these fuels enables the continuous generation of electrical energy.

The market for fuel cells is strong and growing every day [7]. As an integrated and functional device, they were initially used in space vehicles. There, hydrogen and oxygen were used as a reducer and oxidant, which in its chemical reaction produces water as a residue, which was used both by the astronauts and by the vehicle itself as part of its cooling system. Today its use has not become widespread due to its cost, which is higher than other sustainable technologies. Even so, its development is continuous, and has in the market products of great impact [8]. Honda, for example, has approval in the United States and Japan for the use of fuel cells in its vehicles. There are also commercial systems for domestic use (the home energy station (HES), for example) that produce hydrogen from natural gas for electric power generation.

The first prototypes of fuel cells date back to 1838 with the work of Christian Friedrich Schönbein and Sir William Grove with gaseous batteries [9-11]. However, interest in their development has been pressured by the shortage of energy resources, which has not been common throughout these last two centuries. Today there is a great interest in development also driven by strong ideas of sustainable energy sources and less dependence on petroleum. The current prototypes are focused on two categories: batteries for portable applications and batteries for non portable applications. The sizes and uses are wide, and can be found in small capacity for mobile phones or high capacity for buildings or even submarines.

One of the most common fuel cell architectures is the proton exchange membrane (PEM) [12, 13]. This battery uses a water-based, acidic polymer membrane as electrolyte, and two platinum-based electrodes. The electrolyte functions as an electrical insulator between the electrodes, and a medium for the reactions that occur from the anode (where the fuel is oxidized) to the cathode (where the oxidant is reduced). The electrons move from the anode to the cathode with the help of an external circuit, which constitutes the flow of electric current and the difference in potential energy between the two electrodes. Internally the positive charges are displaced through the electrolyte as shon in Figure 1. The reaction is slow, so a catalyst is used to control it, and it produces heat (usually operating below 100 degrees celsius). The scheme shown in Figure 1 corresponds to a cell, these are usually grouped (50 or more) in series and/or parallel to increase the voltage and power output values.

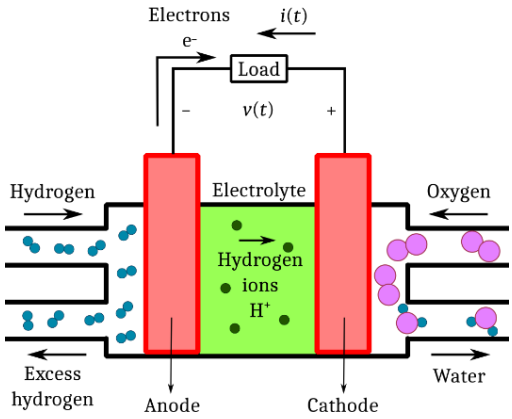

Figure 1. Simplified structure of a proton exchange membrane (PEM) cell

An energy supply system based on fuel cells requires, in addition to the battery, other elements for the handling and conditioning of gases, liquids and the final electrical energy as shown in Figure 2, these elements are known as balance of plant (BOP) [14, 15]. In a first stage there is the reformer, in charge of transforming the input fuel (hydrogen, and natural gas) into a hydrogen-rich gas with traces of carbon monoxide. After the reformer, the gas is subjected to a purification process, and finally it is injected into the fuel cell. The fuel cell generates the electrical energy, and this energy is injected into an energy conditioning system, which regulates the voltage and power according to the final application [16, 17]. This energy conditioning system consists mainly of a power converter, which must be designed taking into account both the operation of the fuel cell and the power requirements of the load.

The cost of a fuel cell is usually high due to the high cost of the catalyst [18]. However, in isolated and difficult to access places such as weather stations, natural parks and rural towns not connected to the power system, they are a viable and economical solution compared to other alternatives. In many cases, it is even economical in cogeneration systems [19]. This is because the fuel cell-based system is compact, can be fed with fuels from the point of operation, requires less maintenance, and has a very high reliability (practically no moving parts, and does not use combustion). In mobility applications, fuel cells have been implemented in prototype vehicles, buses, forklifts, motorcycles, bicycles and even airplanes, boats and submarines [20]. In this sector it is still a developing technology that competes with other more mature technologies.

We propose the development of an electric power conditioning system for energy supply applications based on formic acid fuel cells (direct formic acid fuel cells or DFAFCs) for low and medium power applications (up to 25 W) suitable for small portable applications (such as laptop computers) as well as larger fixed power applications and small vehicles, characterized by high performance and low cost [21-23]. DFAFCs are a very attractive alternative for the development of power supply systems given their comparative advantages such as high in electromotive force and low fuel crossover [24-26]. In that sense, we use a boost converter operating in continuous conduction mode (CCM) as power topology, and a digital control unit based on the ARM Cortex-M3 CPU [27, 28]. A static neural network trained with the non-linear behaviour of the power converter was used as a control strategy.

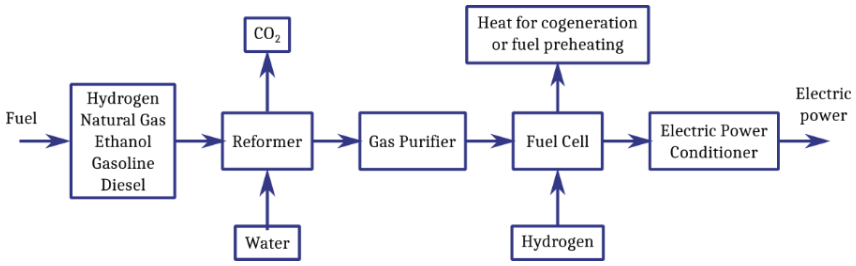

Figure 2. Elements that compose a balance of plant (BOP)

2. MATERIALS AND METHODS

2.1. Problem Formulation

The output voltage at the terminals of the fuel cell is continuous voltage or direct current (DC). Our prototype is designed for 5 DFAFC cells of 21x30 cm each connected in series. This connection provides a terminal voltage of 3.6 Vdc. The maximum estimated output power is 25 W, and the final load corresponds to small electronic devices, so the output voltage is set at 5 Vdc. According to these conditions, and considering the performance and cost of the system, the boost regulator is selected as the power topology. The boost regulator is a DC-DC converter capable of delivering a DC voltage always higher than the input DC voltage as shown in Figure 3. It is a high-efficiency circuit that works by high-frequency switching, supporting the transfer and voltage rise in an inductive element called choke (L). The switching is controlled by a controlled semiconductor switch (transistor, denoted by Q), supported by an uncontrolled semiconductor switch (diode, denoted by D). Also, to ensure continuity of the output voltage, the circuit normally uses a capacitor as a filter (C_0). Since the output has a diode, the output current is discontinuous (and therefore the voltage on the load) if this capacitor is not used. Therefore, the design of the capacitor is linked to the power consumed by the load and the voltage ripple allowed on it.

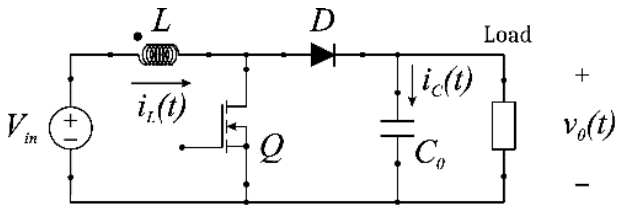

Figure 3. Boost converter, selected power topology for the system

Due to the switching, the operation of the boost converter is characterized by two states, and its dynamics is of a non-linear type. If the load is resistive (i.e. linear, which even in case it is not, can be emulated by handling the Q switching), the operation of each of these two states, originated by the conductive or ON state of the transistor, and the non-conductive or OFF state of the transistor, can be easily analyzed as shown in Figure 4. When the transistor Q is closed (ON-state), and assuming that ideally, it behaves as a short circuit, the energy delivered by the fuel cell is stored in the choke (which is designed not to get saturated with DC), while the output capacitor is discharged through the load (this is the design parameter of the capacitor). When the Q transistor is OFF-state, the only available path for the current is through the diode, charging the capacitor and feeding the load.

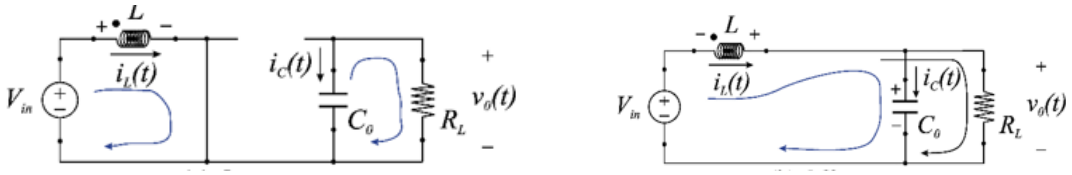

Figure 4. Switching states of the boost converter; (a) on- State: The transistor is activated and energy is stored in the choke, (b) off-state: the transistor is deactivated and the energy of the choke is transferred to the load

The complex part of this circuit is its control due to its non-linear characteristic, and the need to regulate the output ensuring stability [29]. To ensure both voltage regulation and stability it is necessary to feedback both output voltage and output current. Also, the behavior of the current in the choke must be considered, i.e. the behavior of the circuit changes completely if the inductance of the choke is very small, causing it to discharge completely during the OFF-state before starting the ON-state. If the latter case occurs, the converter operates in discontinuous conduction mode (DCM), however, we design the inductance value so that it does not discharge completely, and therefore guarantee continuous conduction mode (CCM). From Figure 4 (a), as shown in (1):

$$L\frac{di_L(t)}{dt} = V_{in}(t) \text{ and } C_0\frac{dv_C(t)}{dt} = -\frac{v_C(t)}{R_L} \quad (1)$$

The switching on and off of the transistor is controlled by pulse-width modulation (PWM). For PWM signal management independent of the switching frequency, f_s (and therefore of the time variable), the duty cycle d is defined as the ratio of the switching time (t_{ON}) to the switching period T ($t = 1/f_s$), i.e. $d = t_{ON}/T$. The control signal on the transistor, $u(t)$, is defined by the average behavior of the converter, as a continuous control signal representing the percentage of the PWM duty cycle. In this way, the average switching of the boost converter is given as shown in (2):

$$\begin{aligned} L\frac{di_L(t)}{dt} &= -\left[r_L + [1-u(t)]^2\frac{r_C R_L}{r_C+R_L}\right]i_L(t) - [1-u(t)]\frac{r_C R_L}{r_C+R_L}v_C(t) + V_{in}(t) \\ C_0\frac{dv_C(t)}{dt} &= [1-u(t)]\frac{R_L}{r_C+R_L}i_L(t) - \frac{v_C(t)}{r_C+R_L} \end{aligned} \quad (2)$$

where r_L and r_C correspond to the parasitic resistances in series of the choke and the output capacitor, and $v_C(t)$ is the voltage over the capacitor, without including its parasitic resistance. The output voltage as shown in (3):

$$v_0(t) = \frac{R_L}{r_C+R_L}v_C(t) + [1-u(t)]\frac{r_C R_L}{r_C+R_L}i_L(t) \quad (3)$$

The output voltage depends on the average value of the duty cycle and the input current. The parasitic resistance of the capacitor limits the ability to raise the voltage of the converter. Besides, the dynamic is non-linear with continuously changing variables. The control must monitor both the output voltage regulation and the input current behavior to ensure the speed of response and stability.

2.2. Methodology

The boost converter was designed to operate in CCM, the critical inductance value for the circuit conditions (25 W output power, 5 Vdc nominal output voltage, and 20 kHz switching frequency) was 3.63 uH, so the choke inductance was chosen to be 5 uH. For an output voltage ripple of 1% (0.05 V), the minimum capacitance value is 280 uF, we use a 300 uF capacitor. The final converter design parameters are summarized in Table 1. Control to output transfer function as shown in (4). Figure 5 shows the frequency response of the boost converter without feedback or control.

$$\frac{V_0(s)}{d(s)} = \frac{V_{in}}{[1-d_0]^2}\frac{1+s\frac{L}{R_L[1-d_0]^2}}{1+s\frac{L}{R_L[1-d_0]^2}+s^2\frac{LC_0}{[1-d_0]^2}} \quad (4)$$

Table 1. Design parameters

Parameter	Value
V_{in}	3.6 Vdc
V_0	5 Vdc
P_0	25 W
V_r	0.05 V
f_s	20 kHz
C_0	300 uF
L	5 uH

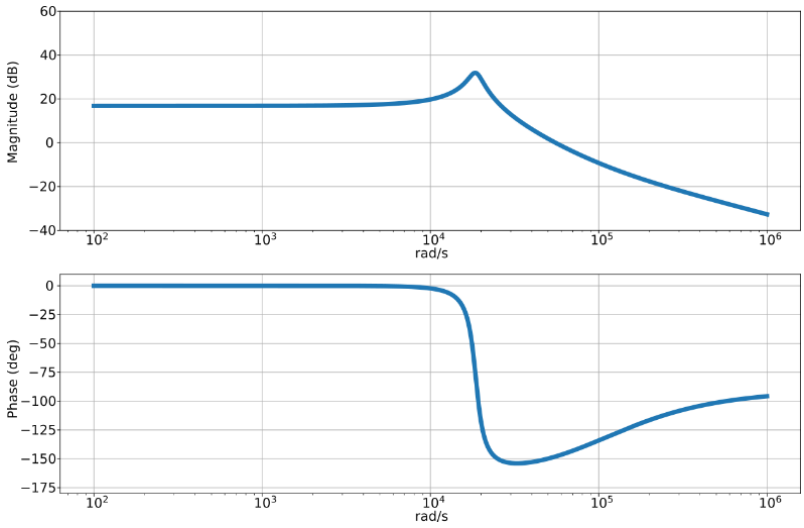

Figure 5. Frequency response of boost converter uncompensated

We propose the use of a neural network to estimate the $u(t)$ control values due to their ability to learn and generalise from previous cases. In addition to its high fault tolerance, after being trained, its operation by propagating the information from the sensors throughout its architecture produces a fast response value (the delays are concentrated in the sampling times of the A/D converters). The training of the neural network was done using data simulated with the model of the converter. Weight optimization was performed using a genetic algorithm. In the genetic algorithm, the values of all the weights were coded as a single chromosome with real values, the genes were randomly selected and the strategy of floating-point mutation was applied to them, and we used a single cross point for recombination. The fitness function was constructed with the step response stabilization time (t_s) and the overshoot voltage (V_{OS}). All training was performed off-line using Python 3 and Keras. We used a feed-forward neural network of size 3-20-20-1 (two hidden layers).

To perform voltage mode control (output voltage regulation), the instantaneous input and output voltages were fed back to the control unit. To ensure stability of the scheme and power management, the input current, i.e. the current in the choke, was also fed back. These three parameters were normalized to their maximum and minimum values in the range of [0, 1] (their average values are always positive). The control scheme was implemented on a 32-bit ARM® Cortex®-M3 PSoC® 5LP. For the computation of these signals we use three 12-bit channels of the microcontroller as shown in Figure 6.

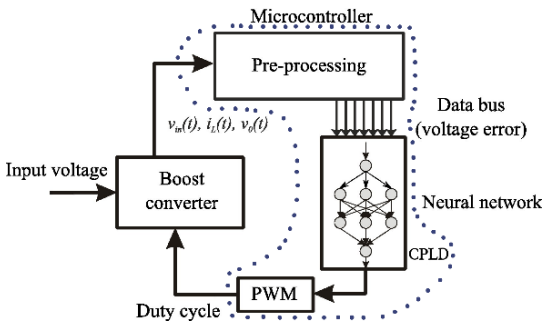

Figure 6. Structure of the control unit. The blue dotted line corresponds to the PSoC 5LP board

The neural network structure was implemented using the digital blocks of the PSoC. Most of the instrumentation (reading of analog signals and calculation of the PWM duty cycle) was performed in the microcontroller as shown in Figure 6. The design was made as simple as possible, considering both the lowest cost and the highest performance. With the input voltage, input current and output voltage signals the microcontroller calculates the voltage error according to the reference voltage (5 V), and sends the value to the CPLD unit containing the neural network structure. The output of the neural network is used for the calculation of the duty cycle applied to the boost transistor. The protitope was evaluated in the laboratory on a power resistive load with a value of 1 Ω, using a hand-held choke, and a low value power resistor as current sensor.

3. FINDINGS

To evaluate the performance of the conditioning system against changes in load, after the system has reached a steady state, we apply a change in load to emulate the effect produced by instantaneous changes in load, keeping the input voltage and other circuit parameters constant. This effect was produced by varying the load resistance from 1 Ω to 0.5 Ω (another one was connected in parallel with the first one). The system behavior is shown in Figure 7. When the severe load change occurs, the output voltage drops approximately 0.7 V (14% of its value), and then recovers quickly (in approximately 45 ms) maintaining voltage regulation with the new load demand. This demonstrates a high speed of response and robust against abrupt power increases, even with values above its nominal power (at least for a few seconds). Output voltage stability was maintained during testing, even when input voltage to the converter varied.

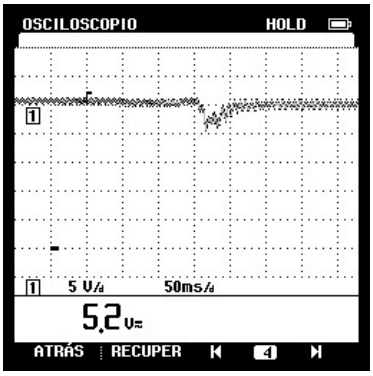

Figure 7. Output voltage (5V/div). The load resistance is changed from 1 Ω to 0.5 Ω

4. CONCLUSIONS

This article presents a power conditioning scheme suitable for low and medium power applications based on DFAFCs. The design assumed the use of 5 DFAFC cells of 21 cm x 30 cm with a nominal power density of 41 mW per cm^2. Presuming its use in small electronic equipment, such as that found in telecommunications equipment, the functional profile of the voltage regulator was defined (power converter design values). With the intention of developing a low cost and high-performance system, we proposed the use of a direct control scheme over the power converter based on a static neural network. This neural network was trained through a genetic algorithm, using the functional values provided by its average model. The converter has a complex and non-linear dynamics, so to guarantee regulation and stability, feedback was performed on both the output voltage and the input current (internal and external loop). The whole control scheme was programmed inside a 32-bit ARM® Cortex®-M3 PSoC® 5LP. The 32-bit microcontroller was used for instrumentation, processing and calculation of the PWM control signal, while digital blocks were used to implement the neural network. During laboratory testing of the prototype, excellent response and regulation to changes in load was observed, these tests were performed by doubling the current requirement as a load step (5 A to 10 A).

ACKNOWLEDGEMENTS

This work was supported by the Universidad Distrital Francisco José de Caldas, in part through CIDC, and partly by the Facultad Tecnológica. The views expressed in this paper are not necessarily endorsed by Universidad Distrital. The authors thank the research group ARMOS for the evaluation carried out on prototypes of ideas and strategies.

REFERENCES

[1] P. Edwards, V. Kuznetsov, W. David, and N. Brandon, "Hydrogen and fuel cells: Towards a sustainable energy future," *Energy Policy*, vol. 36, no. 12, pp. 4356-4362, December 2008.

[2] N. Rees and R. Compton, "Sustainable energy: a review of formic acid electrochemical fuel cells," *Journal of Solid State Electrochemistry*, vol. 15, no. 1, pp. 2095-2100, October 2011.

[3] W. Li, H. Yu, and Z. He, "Towards sustainable wastewater treatment by using microbial fuel cells-centered technologies," *Energy & Environmental Science*, vol. 7, no. 3, pp. 911–924, March 2014.

[4] R. Nitisoravut and R. Regmi, "Plant microbial fuel cells: A promising biosystems engineering," *Renewable and Sustainable Energy Reviews*, vol. 76, no. 1, pp. 81–89, September 2017.

[5] L. An and T. Zhao, "Transport phenomena in alkaline direct ethanol fuel cells for sustainable energy production," *Journal of Power Sources*, vol. 341, no. 1, pp. 199-211, February 2017.

[6] A. Abdalla, S. Hossain, A. Azad, P. Mohammad, F. Begum, S. Eriksson, and A. Azad, "Nanomaterials for solid oxide fuel cells: A review," *Renewable and Sustainable Energy Reviews*, vol. 82, no. 1, pp. 353–368, February 2018.

[7] D. Niakolas, M. Daletou, and S. Neophytides, "Fuel cells are a commercially viable alternative for the production of clean energy," *Ambio A Journal of the Human Environment*, vol. 45, no. 1, pp. 32-37, December 2015.

[8] Z. Cano, D. Banham, and S. Ye, "Batteries and fuel cells for emerging electric vehicle markets," *Nature Energy*, vol. 3, no. 4, pp. 279-289, April 2018.

[9] C. Santoro, C. Arbizzani, B. Erable, and I. Ieropoulos, "Microbial fuel cells: From fundamentals to applications. a review," *Journal of Power Sources*, vol. 356, no. 1, pp. 225-244, July 2017.

[10] S. Joshi and D. Rai, "Design and simulations of solid oxide fuel cell connected to 3-phase electrical power system," *International Journal of Scientific Research in Computer Science and Engineering*, vol. 5, no. 6, pp. 75–78, 2017.

[11] M. Yurukcu, E. Badradeen, S. Bilnoski, F. Yurtsever, and M. Begum, "The effect of the core/shell nanostructure arrays on PEM fuel cells: a short review," *Material Science & Engineering International Journal*, vol. 2, no. 2, pp. 58–64, April 2018.

[12] A. Gago, *et al.,* "Protective coatings on stainless steel bipolar plates for proton exchange membrane (PEM) electrolysers," *Journal of Power Sources*, vol. 307, pp. 815–825, March 2016.

[13] M. Sauermoser, N. Kizilova, B. Pollet, and S. Kjelstrup, "Flow field patterns for proton exchange membrane (PEM) fuel cells," *Frontiers in Energy Research*, vol. 8, no. 13, pp. 1-20, February 2020.

[14] C. Merino and D. Hidalgo, "Open source hardware for pem fuel cells control," *Electrical & Electronic Technology Open Access Journal*, vol. 1, no. 1, pp. 29-31, 2017.

[15] R. Winter, P. Singh, M. King, M. Mahapatra, and U. Sampathkumaran, "Protective ceramic coatings for solid oxide fuel cell (SOFC) balance-of-plant components," *Advances in Materials Science and Engineering*, vol. 2018, 2018.

[16] G. Avgouropoulos, *et al*., "Performance evaluation of a proof-of-concept 70 w internal reforming methanol fuel cell system," *Journal of Power Sources*, vol. 307, pp. 875–882, March 2016.

[17] A. Ferriz, A. Bernad, M. Mori, and S. Fiorot, "End-of-life of fuel cell and hydrogen products: A state of the art," *International Journal of Hydrogen Energy*, vol. 44, no. 25, pp. 12 872–12 879, May 2019.

[18] J. Choulder, *et al.,* "Exploring the use of cost-effective membrane materials for microbial fuel cell based sensors," *Electrochimica Acta*, vol. 231, pp. 319–326, March 2017.

[19] V. Dhulipala, R. Gurjar, and M. Behera, "Bioelectricity generation from kitchen waste in a low-cost earthenware microbial fuel cell," *Lecture Notes in Civil Engineering*, vol. 57, no. 1, pp. 309-322, 2018.

[20] A. Alaswad, A. Baroutaji, H. Achour, J. Carton, A. Makky, and A. Olabi, "Developments in fuel cell technologies in the transport sector," *International Journal of Hydrogen Energy*, vol. 41, no. 37, pp. 16499-16508, October 2016.

[21] C. Rice, *et al.,* "Direct formic acid fuel cells," *Journal of Power Sources*, vol. 111, no. 1, pp. 83–89, September 2002.

[22] X. Yu and P. Pickup, "Recent advances in direct formic acid fuel cells (DFAFC)," *Journal of Power Sources*, vol. 182, no. 1, pp. 124-132, July 2008.

[23] S. Ha, R. Larsen, Y. Zhu, and R. Masel, "Direct formic acid fuel cells with 600 mA cm-2 at 0.4 V and 22 oC," *Fuel Cells*, vol. 4, no. 1, pp. 337–343, December 2004.

[24] N. Aslam, M. Masdar, S. Kamarudin, and W. Daud, "Overview on direct formic acid fuel cells (DFAFCs) as an energy sources," *APCBEE Procedia*, vol.3, pp. 33–39, 2012.

[25] I. Al-Akraa, A. Mohammad, M. El-Deab, and B. El Anadouli, "Advances in direct formic acid fuel cells: Fabrication of efficient Ir/Pd nanocatalysts for formic acid electro-oxidation," *International Journal of Electrochemical Science*, vol. 10, no. 4, pp. 3282–3290, February 2015.

[26] G. Nagar, M. Hassan, and I. Lauermann, "Efficient direct formic acid fuel cells (DFAFCs) anode derived from seafood waste: Migration mechanism," *Scientific Reports*, vol. 7, no.1, pp. 1–11, December 2017.

[27] F. Martínez, C. Hernández, and E. Jacinto, "Rectificador de alto desempeño para aplicaciones de media potencia en equipos con alimentación universal," *Revista Tekhnê*, vol. 10, no. 1, pp. 19–27, 2013.

[28] Y. Ochoa, J. Rodríguez, and F. Martínez, "Low cost regulation and load control systemfor low power wind turbine," *Contemporary Engineering Sciences*, vol. 10, no. 28, pp. 1391–1399, January 2017.

[29] F. Martínez, F. Martínez, and E. Jacinto. "Strategy for the Selection of Reactive Power in an Industrial Installation Using K-Means Clustering," *Communications in Computer and Information Science*, vol. 1071, pp. 146-153, July 2019.